

# System Design Process of a Whale Scouting Small Unmanned Aircraft System

Grant Dunbar\* and Benjamin J. Mellinkoff†

*CU Boulder Ann and H.J. Smead Aerospace Engineering Sciences, 429 UCB, Boulder, CO 80309-0429, USA*

Severyn V. Polakiewicz‡

*CU Boulder Ann and H.J. Smead Aerospace Engineering Sciences, 429 UCB, Boulder, CO 80309-0429, USA*

The University of Colorado-Boulder senior design team, Search and Help Aquatic Mammals sUAS (SHAMU), is developing a shipborne, small unmanned aircraft system (sUAS) designed to increase the whale-searching capabilities of the Cetacean Echolocation Translation Initiative (CETI). The SHAMU sUAS is required to launch, operate, and be recovered from a 9.1 m square helipad on a research vessel. On flight missions, the sUAS will capture aerial photography useful to marine biologists in locating whales. The sUAS will support a payload of 2 kg to accommodate instruments responsible for sensing whales in the ocean below. CETI requires that the sUAS be capable of covering a 100 km ground track at 70 km/h to provide an effective search area around the research vessel. Additional requirements were also imposed, such as a maximum aircraft weight of 22.7 kg, modular design for ground turnarounds of under 30 minutes, and an electric propulsion system. In addition to the development of the sUAS, a launch and recovery system is being developed in order to operate the sUAS from the specified helipad. Designing a new aircraft from scratch was chosen over purchasing an existing aircraft to achieve the mission requirements detailed by CETI while remaining within a budget of \$5000. The methods and design process of the sUAS are described, including sizing considerations of an all-electric aircraft designed to meet the specific range, payload mass, and endurance requirements.

## I. Nomenclature

$AR$	=	aspect ratio
$C_{D_i}$	=	induced drag coefficient
$C_L$	=	lift coefficient
$C_{L_{max}}$	=	max lift coefficient
$E_{losses}$	=	energy losses due to friction and gravity
$e$	=	span efficiency
$f$	=	force of friction
$k$	=	spring constant
$m_{comb}$	=	combined mass of aircraft and dolly
$\rho$	=	air density
$S$	=	wing area
$V$	=	air speed
$V_d$	=	dolly velocity
$V_S$	=	stall speed
$W$	=	aircraft weight
$X_i$	=	initial length of bungees
$x$	=	distance

---

\*Aerospace Engineering Undergraduate, Ann and H.J. Smead Aerospace Engineering Sciences, 429 UCB, Boulder, CO 80309-0429, USA

†Aerospace Engineering Undergraduate, Ann and H.J. Smead Aerospace Engineering Sciences, 429 UCB, Boulder, CO 80309-0429, USA

‡Aerospace Engineering Undergraduate, Ann and H.J. Smead Aerospace Engineering Sciences, 429 UCB, Boulder, CO 80309-0429, USA

## II. Introduction

THE Search and Help Aquatic Mammals sUAS (SHAMU) senior design team at the University of Colorado-Boulder is designing and developing a fixed-wing, small unmanned aircraft system (sUAS) to assist in locating sperm whales in the ocean. The SHAMU team is developing the sUAS to help the Cetacean Echolocation Translation Initiative (CETI) in their efforts to decode the click-communication used by sperm whales. CETI utilizes the whales' locations to deploy auditory and visual buoys, which record the clicking and associated behavior of the whales. By collecting a large sample of whale social clicks, CETI hopes to understand whale communication patterns to promote whale conservation and deter cetaceans away from dangerous areas.

Currently, CETI's primary method for locating sperm whales is to equip marine biologists with binoculars. Marine biologists search the waters surrounding their research vessel for surfacing whales and water spouts. This method of locating sperm whales is prohibitively costly and relatively inefficient. CETI has decided that operating a whale-scouting sUAS would decrease the cost, increase the effectiveness of locating whales from a research vessel, and increase the return on investment to promote research funding. CETI's ideal sUAS would be an autonomous aircraft with an onboard sensor payload capable of identifying whales in the ocean below. Once the sUAS identifies whales, the GPS coordinates of the identified whales would be sent to the research vessel, where a small manned boat would depart towards the whales' location.

CETI provided requirements of the sUAS to ensure that the delivered product would increase the effectiveness of locating whales from a research vessel. CETI required that the sUAS be capable of taking off and landing on a 9.1 m x 9.1 m platform that is obstructed fore and aft. This is to accommodate operations from the research vessel's helipad. The sUAS is required to fly at 70 km/h for 1.4 hours to achieve a ground-track range of 100 km. The purpose of this requirement is to increase the chance of locating whales by providing a sufficient search area. While the sUAS shall have a 100 km ground-track range, CETI has required that the sUAS have a maximum displacement from the research vessel of 12 km. Whales surfaces for about an hour, which limits the distance that the dispatched vessel can travel before the whales have moved to a different location. CETI requires that the sUAS be modular so that damages to the sUAS can be fixed within 30 minutes by using replacement components. The sUAS shall support a downward facing payload bay to enable autonomous detection of whales. The sUAS shall transfer images and GPS coordinates to the ground station. Lastly, CETI has required that the sUAS can be no heavier than 22.7 kg and must have an electric propulsion system. Section III: Project Scope will discuss the scope of SHAMU's project, Section IV: Design Solution will discuss the design of the sUAS, and Section V: Next Steps will discuss future work for our project.

## III. Project Scope

CETI's final deliverable has three main components: the sUAS, the autonomous whale sensing payload, and an optimized whale-searching flight path. The sUAS itself is composed of three major sub-systems: the aircraft, the launch system, and the recovery system. Figure 1 shows the concept of operations (CONOPS) for the final deliverable. This CONOPS shows all of the steps for an operational flight. The aircraft, take-off system, recovery system, and communications ground station are all assembled on-board the research vessel. Once assembled, the sUAS is launched into flight and then begins its autonomous search flight for whales. Note that the yellow circle in Fig. 1 only represents the maximum displacement from the research vessel and does not necessarily represent the shape of the flight path. Once the sUAS's whale-sensing payload identifies a whale, the GPS coordinates and image will be transmitted to the research vessel. The sUAS will be recovered on the research vessel once the flight is complete. The battery and any damaged modular components will be changed if it is desired to fly the aircraft again.

The SHAMU team will only be engineering the sUAS for the 2017-18 academic year. The whale-sensing payload and the optimized search path will be engineered in future years using a future senior design team. This decision was made due to the large scope of the full project, which would be challenging to accomplish with a 12 member team confined to the schedule of the academic year. The CONOPS for this year is similar to the CONOPS shown in Fig. 1, however the sUAS will not be actively looking for a whale. In fact, the aircraft will not be operating over an ocean this year. The aircraft will be flown over ground, however the launch/recovery will be constrained to a 9.1 m x 9.1 m area. The CONOPS for this year will be done primarily to test the launch/recovery systems, the range and endurance of the aircraft, and the range of the communication systems.

The critical project elements (CPEs) were selected as the driving requirements to ensure the success of the project. The SHAMU team has four CPEs: Aerial Vehicle, Launch and Recovery, Communication with Ground Station, and Flight Computer / Autopilot. The Aerial Vehicle CPE is concerned with the stability, control, and endurance of the aircraft. The Launch and Recovery CPE is concerned with launching and recovering the aircraft from a 9.1 m x 9.1 m

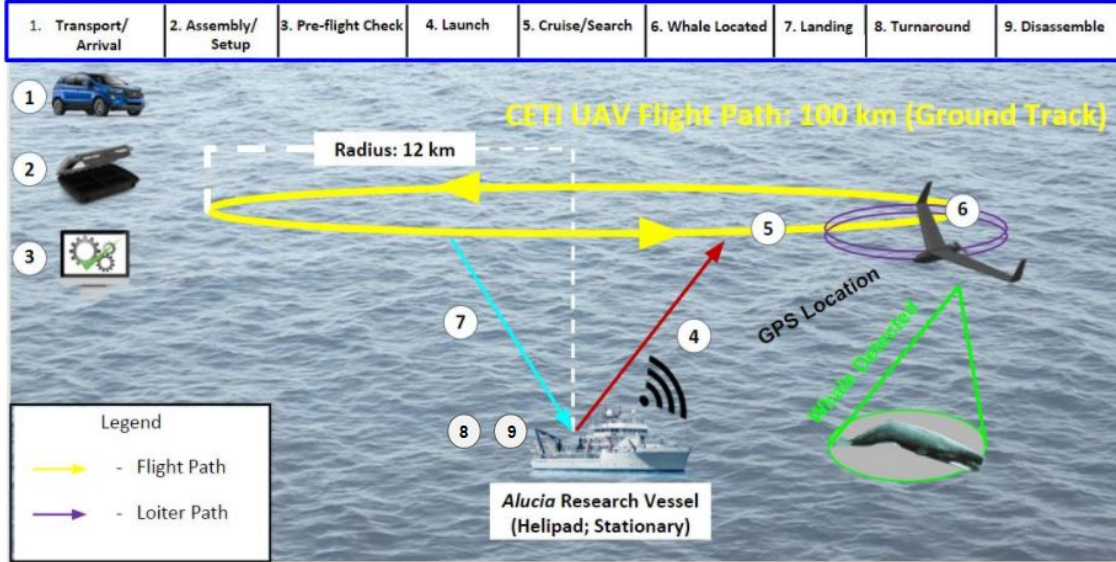


**Fig. 1 CONOPS for Final Deliverable**

area without exceeding a 5 g structural limit. This paper will only cover the design considerations for the Aerial Vehicle CPE and the Launch and Recovery CPE.

Once the project was scoped, the SHAMU team began trade studies to determine the design of the aircraft and launch/recovery systems. The main results from the trade studies are as follows: the aircraft will be a fixed-wing with a 3 m wingspan and will be designed and manufactured from scratch. The launch system will be composed of a dolly-rail system powered by bungees. The recovery system will be a collapsible net system designed to capture the sUAS upon recovery. The design of these systems are discussed in detail in Section IV: Design Solution.

## IV. Design Solution

### A. Wing Design

The first parameter of the wing found was the area. The wing area is directly related to the weight (18 lbs) and desired stall speed of the aircraft, which was chosen as 35 ft/s (matching the maximum design winds). A rearranged form of the lift equation was then used:

$$S = \frac{W}{1/2\rho V^2 C_{L_{max}}} \quad (1)$$

Air density was assumed to be 0.002377 slug/ft<sup>3</sup> (sea level air density), as the design mission of the aircraft involves flying in near sea level conditions.  $C_{L_{max}}$  was assumed to be 1.2, thought to be conservative for a high aspect ratio wing operating at relatively low Reynolds numbers (< 500,000). This gives a wing area of approximately 10 ft<sup>2</sup>.

Given that the aircraft must remain on mission for just under one and one-half hours, it is important to reduce drag and maximize L/D. This can of course be done by increasing the aspect ratio to decrease induced drag in accordance with the formula:

$$C_{Di} = \frac{C_L^2}{\pi e AR} \quad (2)$$

Increasing aspect ratio has benefits, however these must be balanced with keeping the aircraft a manageable size. With very large aspect ratios the span of the aircraft gets very large, which requires increased structural strength to cope with the larger wing bending moments as well as increased structural complexity to account for additional dis-assembly points so the aircraft can be effectively transported without specialized equipment. Other aircraft in similar missions to the present one were examined for wing span, including commercial/military UAS such as the Aerosonde and the Insitu

Scan Eagle, as well as long-endurance and glider-type radio controlled aircraft, such as the Thornburg Bird of Time and the Bearospace Gemini V2 [1–4]. In all of these cases the wingspan was limited to approximately 10 ft, and from this the aspect ratio of the aircraft was set at 10.0, giving a wingspan of 10 ft.

The next item of consideration in the wing design is the taper ratio. It is well known that the “most efficient” taper ratio in terms of maximizing span efficiency  $e$  is approximately 0.4 (exact estimates vary, but are generally around this number). The taper ratio on this aircraft was set slightly larger at 0.5 in order to facilitate support for wider winglets, as well as make measurements involving the wing chord simpler.

For tapered wings and swept wings it is important that the wing has a measure of washout along its span to ensure that it has adequate stall and spin characteristics. Since data on washout in existing UAS is lacking, the washout values of a selection of full scale aircraft were examined. It was found that 3 degrees of washout was a typical value for a full scale aircraft (with some having more, and some having less), and so 3 degrees of washout was selected for this aircraft.

As the aircraft has a flying wing configuration, the wing sweep is very important in determining the characteristics of the aircraft, significantly shifting the aerodynamic center and varying the control arm the elevons will pitch the aircraft about. A variety of flying wing sUAS aircraft were considered for wing sweep from the SKYwalker X-8 to the Prandtl-3c, and it was found that the quarter chord sweep of these aircraft was typically in the vicinity of 25 degrees. Therefore, the wing sweep of the SHAMU aircraft was set at 25 degrees.

Ordinarily when choosing the wing incidence for an airplane the angle is set such that the fuselage is in a level pitch attitude during cruise. However, for the SHAMU aircraft the wing and fuselage were conceptually designed such that the region of the wing near the root essentially forms a part of the roof of the fuselage. In this configuration adding incidence to the wing would require the fuselage to change height along its length to accommodate the wing. Additionally, since the aircraft has no requirements to be in a level attitude in cruise flight (as would be the case when carrying passengers, for example) the incidence was simply set at zero degrees to simplify the construction of the fuselage and the wing-fuselage junction.

## **B. Fuselage Design**

Fundamentally, the role of the fuselage on the SHAMU aircraft is threefold: it contains the flight electronics (including the motor), the payload, and the recovery hook. The required payload volume for the aircraft is 6 inches by 6 inches by 9 inches. Thus, 6 inches by 6 inches became the internal fuselage cross-section to keep the frontal area of the fuselage to a minimum. Without knowing the exact volumes required for the flight electronics, they were considered to take up an equivalent 6 inches by 6 inches by 9 inches. Thus, the section of the fuselage holding the payload and flight electronics became a rectangular prism measuring 6 inches by 6 inches by 18 inches, with a nose section on the front and a tail section at the rear. The propulsion system was selected as a pusher to avoid the propeller and motor being the first components of the aircraft to strike the net upon recovery, and so the tail section was given the added function of supporting the propulsion system. The nose section was given a square cross-section in order to match the shape of the payload and electronics bays, and was given a 2-caliber tangent ogive shape (resulting in a 12 inch long nose), which is commonly used on rockets for its low-drag performance. The tail section was given a similar shape, but was cut off 6 inches rear of the base in order to facilitate attachment of the propulsion system. The walls and floor of the fuselage were reinforced on the inboard section with balsa wood, and on the outboard section with a continuous piece of fiberglass. The payload bay section of the fuselage was designed to accommodate the mass and volume of a future whale sensing camera payload. The SHAMU team will be utilizing a downward facing Raspberry Pi to send images to the ground station at a rate of one per minute. Note that the hardware and software on-board the SHAMU aircraft does not have the ability to automatically detect whales.

## **C. Powerplant Design**

The aircraft’s powerplant design is driven by the range and speed requirements given by CETI. The aircraft is required to cover 100 km at 70 km/h, which requires 1.4 hours of flight time. From these requirements, the team deduced the aircraft would need a motor powerful enough to reach the required speed and a power source that can last the flight time. To determine the motor power needed, the team performed a steady level flight analysis in which the required power is the thrust force multiplied by the required speed, and the thrust force is equal to the drag of the aircraft. The drag of the aircraft was estimated based on the lift-to-drag ratio of the aircraft and the lift force is equal to the weight of the aircraft. From this process, the required power at steady level flight is 200 watts. Based on this computation, the team chose the Propdrive 5060 motor, which is capable of up to 1500 watts. The reason for a motor with 7 times the required power is to accommodate a climb rate of 5 m/s, which was not a given requirement, but a design choice

by the team. The next step was determining a power source that would last the 1.4 hour flight time. The team listed all the electrical components used by the aircraft, their voltage and amperage requirements, and compiled a power budget to estimate the amount of watt-hours that would be used. The estimation, which included a 10% margin, was approximately 375 watt-hours. The battery chosen is the Tattu-Plus 22000mah 22.2V battery which had an available energy of 390 watt-hours. The propeller chosen was a 16 inch diameter propeller with 8 inch pitch. The Propdrive motor, Tattu-Plus battery, and 16 x 8 inch propeller is the powerplant solution for the aircraft.

#### D. Launch System Design

The launch system consists of rail guided framework and a dolly. The configuration is similar to a roller coaster in that the dolly will move along the rails until the dolly reaches a velocity of  $1.2 V_S$ , approximately 13.2 m/s, within the desired helipad size, 9.1 m. The velocity is derived from the stall requirements of the aircraft design. The dolly is accelerated via rubber bungees that attach to the front crossbeam of the dolly. These bungees are staked into the ground fore of the rail framework. To restrict the dolly from impacting the end of the rail framework a restraining rope attaches to the rear crossbeam of the dolly. The restraining rope will stake into the ground aft of the rail framework.

##### 1. Bungee & Rail Design

The design of the rail system was driven by the spring constant of the bungee and the weight of the dolly. The design model utilizes the basics of conservation of energy to predict the needed spring constant to deliver the aircraft to the required speed of 13.2 m/s. Since the bungee is anchored on the ground at the end of the ramp, the bungee force will not be parallel to the ramp as the aircraft moves up the ramp. There is a component directly parallel with the rails but also a normal component causing an extra load on the ramp. Since the weight of the dolly is known, and the effective bungee force normal to the ramp, the maximum rail deflection can be modeled. In addition, the reaction forces on each fixed support can be calculated. The final design driver is the ability to transport the rails; therefore, making the rails modular. The rails will be cut into 1.68 m segments.

Table 1 refers to the final specifications of the ramp system and Fig. 2 is the model of the rail system with the bungees.

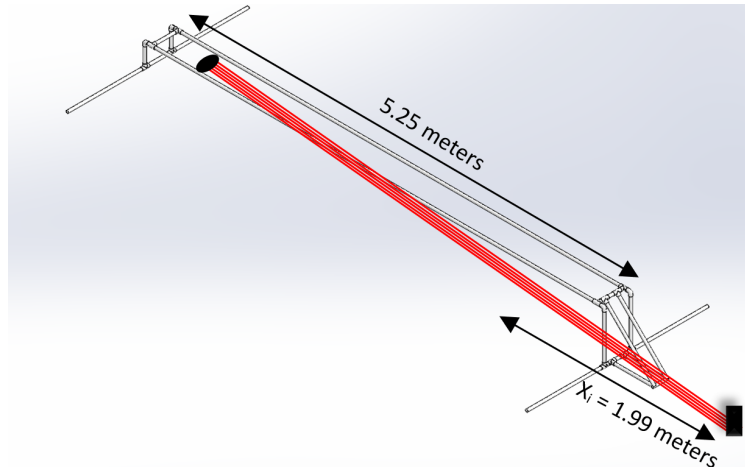


**Fig. 2 Rail System Final Design**

The launcher's ability to accelerate the aircraft above stall speed is critical to project success in order to test the aircraft's flight functions. The analysis begins with the conservation of energy. Note friction and gravity were accounted for when performing the analysis. The final derived equation is shown in Eq. 3.

$$k = \frac{m_{comb} V_d f^2 + 2E_{losses}}{x^2} \quad (3)$$

Note in Eq. 3, the energy losses come from the friction in the wheels and gravity. This value is mitigated by the cradle design with a coefficient of friction of 0.0018 between the bearings of the wheels. It also important to note, the mass  $m_{comb}$  does account for the full weight of the aircraft and the manufactured dolly, (13.96 kg). In order to

**Table 1 Specifications of the Launch Ramp and Bungee System**

Parameter	Value
Ramp Length	5.25 m
Combined Force of Bungee	343 N
Stretch of Bungee	3.99 m
Spring Constant	86.0 N/m
Number of Bungees	5.00
Number of Sections	4.00

calculate a reasonable spring constant, the value  $x$ , or the change the length of the bungee once stretched, must be varied between 0.1 m and the requirement of 9.1 m. The plot of this result is shown in Fig. 3. Every design point selected on this line will give the final launch velocity of 13.2 m/s. The process of selecting the design point will involve evaluating the capabilities of a silicone rubber bungee.

The primary motivation for choosing the silicone rubber bungee was because of its capabilities. The bungee stretch distance was varied between 0.1 m and 9.1 m, and it was overlapped on Fig. 3 using 5 of these bungees in parallel. Note the intersection point of this plot means the specific bungee can get the spring constant, detailed on the y-axis, required to get the aircraft to 13.2 m/s. This is shown in Fig 3.

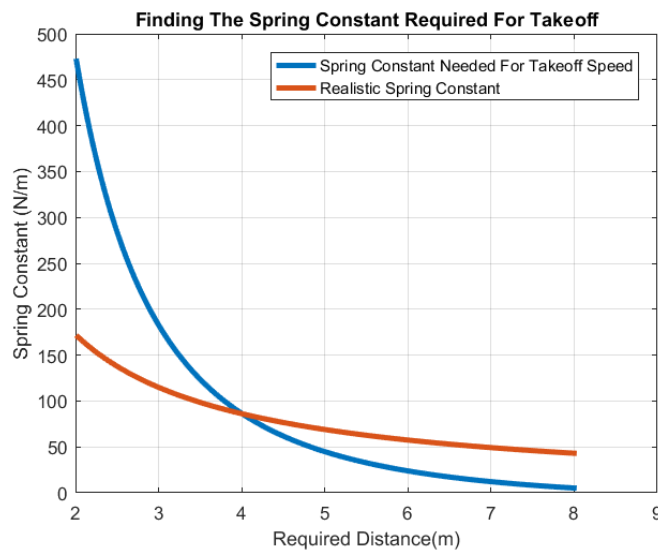


**Fig. 3 Silicone Rubber Capabilities and Required Takeoff Velocity Spring Constants**

## 2. Restraining Rope & Dolley Design

The dolly includes three major sections that are crucial to its design and to a successful launch. The three sections are defined as the aircraft wing slots, the framework, and the wheelbase. The overall weight of the dolly is designed to be as minimal as possible to reduce the amount of force required from the bungees during launch.

The framework of the dolly is the most significant design driver. The goals of the design are to provide the aircraft enough space to fit within the dolly, but not too much that the dolly would slide off axis during launch (dimensions will be discussed later), and the dolly must have a low center of gravity to avoid toppling off the rails during launch. The length of the dolly is driven by the chord of the wings at the root; root chord length is approximately 41 cm. The width of the dolly is driven by the width of the fuselage; fuselage width is approximately 18 cm.

The lower segment of the aircraft wing slots are designed to support the entirety of the wings root chord length; where as the upper segments are designed to hold the aircraft down until the aircraft has reached  $1.2 V_S$  and the dolly

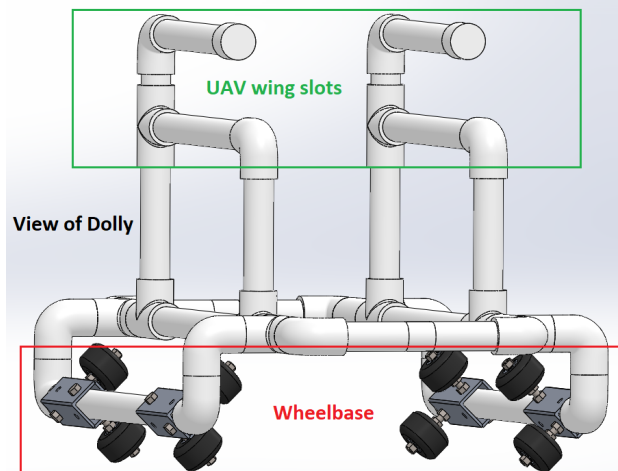


**Fig. 4 View of the dolly**

has reached the end of the rails. The top segments of the aircraft wing slots are at a length such that it holds the wings down at the wing's max thickness (approximately 5 cm). The max thickness of the wing occurs at 12% of the root chord; that is at approximately 10 cm from the leading edge of the wing.

The wheelbase width and length is circumference of the dolly's dimensions. The wheel layout; however, is designed such that the forces felt on the dolly during launch restrict the dolly from falling off the rails.

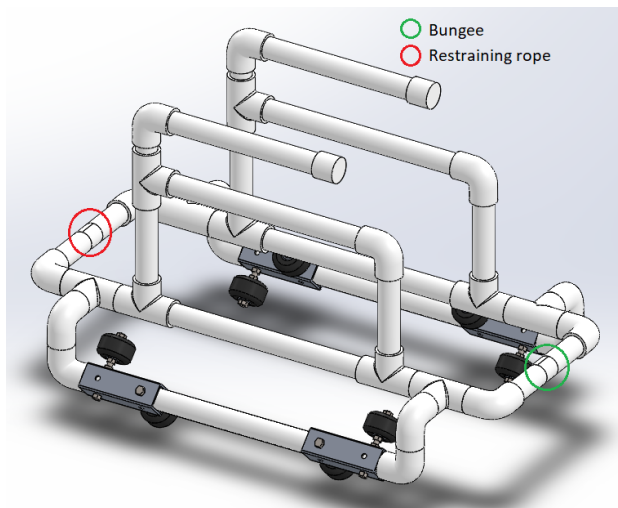


**Fig. 5 View of the dolly demonstrating the connection points for the bungees and restraining rope.**

The white material seen in Fig. 4 is 1 in. Schedule 40 PVC. PVC was chosen due to its high tensile strength and low weight. The crossbeams seen in Fig. 5 will take the load of forces from the bungees and the restraining rope. Therefore, to reduce the distance between the dolly framework and provide space for the aircraft fuselage to fit in the framework the dolly crossbeams are approximately 23 cm. At 23 cm the amount of force with a factory of safety of 2 (chosen by the team) this PVC segment can withstand 1700 N with an expected displacement of approximately 1.5 mm. Both values were found via finite element analysis in SolidWorks [5].

The gray, box-like segments on the wheel base of the dolly seen in Fig. 4 are aluminum angles. These angles provide sturdiness for the PVC so that the wheels remain rigid during launch. Moreover, these aluminum angles lower the center of gravity of the dolly to further restrain the dolly from wanting to tip during launch.

The PVC segments are held together with 1 inch Schedule 40 PVC connectors and PVC cement. PVC cement is designed to hold approximately 7500 N; therefore, for the maximum 1700 N the dolly experiences during launch PVC

cement will keep the dolly together [6].

**Table 2 Dolly design parameters.**

Parameter	Value
Dolly length	82.84 cm
Dolly width	49.87 cm
Dolly height	48.24 cm
Dolly weight	5.90 kg
Wing slot height	6.40 cm
Distance between wing slots	23.28 cm
Length of lower wing slot segment	38.54 cm
Wheelbase width	29.50 cm
Wheelbase length	51.61 cm

The restraining rope material is chosen such that the dolly will experience a near immediate halt. A stiffer material, known as low stretch rope, is required to create this halt. Low stretch rope provides a 6% - 10% elongation. Assuming maximum elongation happens on a 5 meter rail segment the dolly will stop in half of a meter. Using an average impulse force equation a time to stop was calculated. This assumes the maximum tensile strength of PVC with a factor of safety of 2 (1700 N). The time to stop the dolly is approximately 8 hundredths of a second. This halt time is chosen so that the aircraft seamlessly ejects from the dolly. Furthermore, this reduces the amount of rail required for the the dolly by limiting additional rail to a half of a meter.

### 3. Ramp & Dolly Integration

The launch system shall accelerate the aircraft to 13.2 m/s in 9.1 meters. It is critical to the projects success if the speed is achieved. Assuming the results from the previous two sections detailing the dolly and ramp design, a second order speed model was performed to see if it was feasible. Using newtons second law, the driving forces were the effective bungee force, friction and gravity. The plot of the position, velocity and acceleration is below shown in Fig. 6.

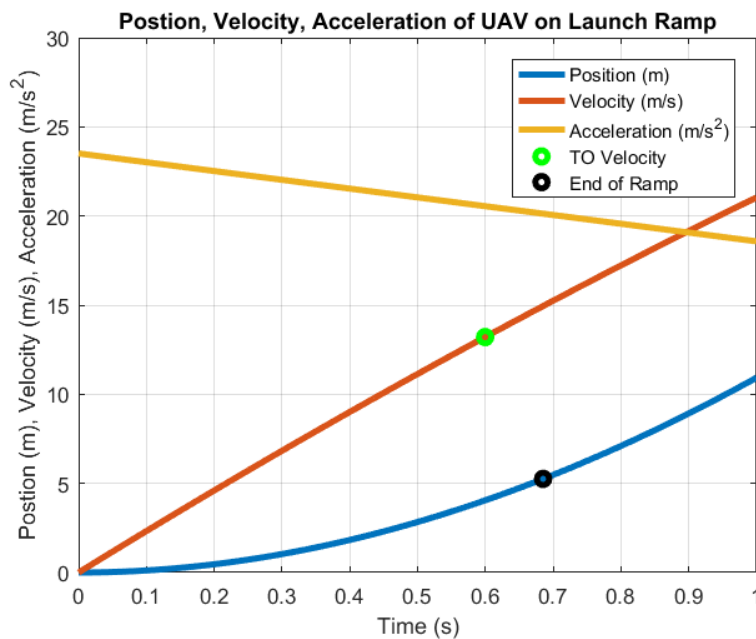


**Fig. 6 Speed model**



It is important to note this only accounts for the aircraft/dolly moving up the ramp to 4 meters, excluding the extra ramp length for the stopping distance of the restraining rope. Shown in the plot, the dolly accelerates the aircraft to 13.2 m/s in 4 meters and the acceleration felt is 1.9 g

### E. Recovery System Design

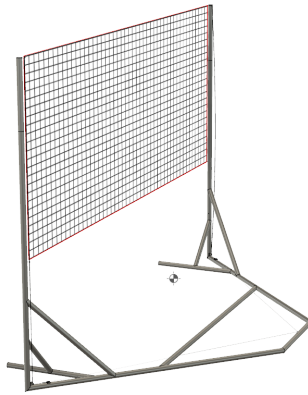


**Fig. 7 Recovery System CAD Model**

The recovery system, shown above in Fig. 7, consists of 2 vertical posts with a net suspended in between them in order to stop the aircraft upon impact. The structure that supports the net and posts is made of PVC to allow for rapid assembly and disassembly of the system and easy storage. The net is attached to a system of bungees and pulleys on the recovery system in order to slow the motion of the aircraft so that it experiences less than 5 g acceleration. In addition, the line attached to the net is run through a sailing cleat to prevent rebound from the bungee after recovery. A plot of the predicted recovery stopping distance and force experienced is shown below in figure 8

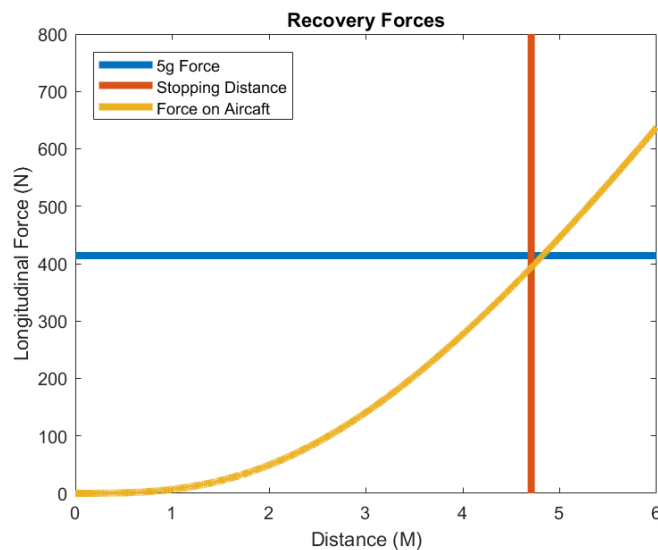


**Fig. 8 Recovery System Predicted Force**

## V. Next Steps

The following section outlines the next steps necessary for a successful project. The section includes future work for the 2017-18 SHAMU team, as well as work for a future senior design team continuing upon the current SHAMU team.

### A. Validation & Verification

The SHAMU team will conduct several validation and verification tests to confirm the main models used in the design phase of the sUAS. There are several validation and verification tests to be completed, however this paper will only cover the three main tests that correspond to the Aerial Vehicle CPE and the Launch and Recovery CPE.

#### 1. Aerodynamics Model Verification

Athena Vortex Lattice (AVL) was the primary aerodynamic software used when designing the aircraft [7]. AVL was used to approximate the lift, stability characteristics, and control surface response of the aircraft. The SHAMU team plans to validate the AVL stability models used in the design phase. There are two main methods for validating the AVL stability model. The first method involves flying a half-scale model of the aircraft with a Pixhawk 2.1 on-board to measure and log the states of the aircraft. The pilot will manually introduce disturbances while flying and the Pixhawk will record the aircraft's response to these disturbances. The collected data will be compared to the predicted response according to AVL's approximated state-space model of the linearized longitudinal and lateral equations of motion. The predicted response will be computed by numerically integrating AVL's state-space models using a set of initial conditions to excite the particular flight mode [8]. The main point of comparison will be the 10% settling times for each of the aircraft's modes. The second method for validating the AVL stability model is identical to the first method, except the full-scale aircraft will be used instead. This method is more risky than using the half-scale, however it is easier to implement because the full-scale is designed to have all of the electronic components necessary for this validation test.

#### 2. Launch System Model Verification

In the design phase, a dynamic model for the speed of the aircraft along the rails was developed using the principles of the conservation of energy. The verification of this model will take place in two stages. First, a representative mass will be launched from the dolly and rails to ensure the system can provide adequate kinetic energy to the aircraft. The required launch speed is  $1.3V_{stall}$ , or  $13.2 \frac{m}{s}$ . The next phase of verification will be launching the SHAMU aircraft from the dolly and rail system. The accelerometer on-board the aircraft will provide data that will be used to directly compare the launch to the models.

#### 3. Recovery System Model Verification

A dynamic model for the force exerted on the aircraft by the landing net was developed in the design phase. The first method of validation for this model uses an accelerometer attached to a representative mass. The mass will be launched into the net at landing speed:  $13.2 \frac{m}{s}$ . The accelerometer data from this test can be used to verify the model, which predicts less than 5 g maximum acceleration, before a test involving the aircraft. Upon completion of a landing during flight testing, the accelerometer data from the aircraft can be used once again for a final verification of the landing model.

### B. Flight Test

After the validation and verification of the main models used in designing the sUAS, a full-scale flight test will be conducted to test the entire sUAS system. The first step in this test is demonstrating that the launch system can launch the full-scale aircraft. Once the aircraft is launched, the aircraft will fly 12 km away to demonstrate the 12 km communications range by transmitting one image from the on-board Raspberry Pi camera. The aircraft will then return and conduct a "figure 8" flight path for the remaining time until a total flight time of 1.4 hours is achieved. The aircraft will have to fly at an average of 70 km/h during this period to achieve the desired 100 km ground track range. After achieving a 1.4 hour flight time, the aircraft will fly into the net for recovery. This will complete the flight test.

### C. Future Years

CETI has scheduled the fully functional sUAS to be a multi-year project with SHAMU as the first year. SHAMU serves as the aerial platform for future instruments that can detect sperm whales in the ocean. An optimized search path will be modelled to maximize whale searching efficiency and increase return on research investment.

### *1. Develop Autonomous Whale Locating Payload*

The SHAMU aircraft has a downward-facing payload bay to accommodate a 2 kg instrument subsystem with 6 inch by 6 inch by 9 inch dimensions. The payload bay specifications are determined by a potential technical solution with conservative masses and sizes. The potential technical solution is comprised of a high-quality, on-board gimballed camera, improved flight computer, and separate battery to power the instrument subsystem for 1.4 hours. The potential camera and flight computer would be capable of processing footage to detect surfaced whales using artificial intelligence. Note that SHAMU has not determined the most suitable whale-detecting design solution through the systems engineering process; however, SHAMU has determined the gimballed camera solution as the potential solution with maximum mass and volume requirements. Another technology for the future team to consider is infrared sensors to identify whale heat signatures. These and other feasible solutions will require an in-depth trade study from the future CETI sUAS team.

### *2. Optimized Search Path*

The SHAMU sUAS has the capability for autonomous flight missions and follows waypoints. These waypoints can be initialized before launch and updated while on mission. SHAMU's scope does not include optimizing the aircraft's search path, which would improve effectiveness in searching for surfaced whales. Thus, a future team will research whale migration patterns and model the path of the sUAS within a 12 km radius of the research vessel. The objective of the model is to determine a search path with highest whale-detection success rate. Inputs to the model are the given 1.4 hour endurance, 100 km ground track range, 70 km/h cruise speed, and capabilities of the future whale sensing payload (field of view, success rate, etc.).

## **References**

- [1] Textron, "Aerosonde Small Unmanned Aircraft System," , 2018. URL <https://www.textron.com/what-we-do/unmanned-systems/aerosonde>.
- [2] Insitu, "ScanEagle Unmanned Aircraft Systems," , 2014. URL <http://www.boeing.com/farnborough2014/pdf/BDS/ScanEagle%20Backgrounder%200114.pdf>.
- [3] Hobbico, "Bird of Time," , 2018. URL <http://www.dynaflite.com/airplanes/gpma1052.html>.
- [4] Bearospace, "Gemini V2," , 2018. URL <http://www.bearospaceindustries.com/give-me-more-data.html>.
- [5] Dassault, 2018. URL [www.SolidWorks.com](http://www.SolidWorks.com).
- [6] TheEngineeringToolbox, "PVC Pipes - Pressure Ratings," , 2018. URL [https://www.engineeringtoolbox.com/pvc-cpvc-pipes-pressures-d\\_796.html](https://www.engineeringtoolbox.com/pvc-cpvc-pipes-pressures-d_796.html).
- [7] Drela, M., 2017. URL <http://web.mit.edu/drela/Public/web/avl/>.
- [8] MathWorks, 2018. URL <https://www.mathworks.com/products/matlab.html>.